Title: Application of numerical simulation to improve efficiency of a sperm sorter

Keywords: Sperm soerter, microfluid, numerical simulation

T. Hyakutake*, Y, Hashimoto*, S. Yanase*, K. Matsuura** and K. Naruse**

*   Graduate School of Natural Science and Technology, Okayama University, Okayama
** Graduate School of Medicine, Dentistry and Pharmaceutical Sciences, Okayama University, Okayama

Abstract

This paper describes a study in which a numerical simulation was used to improve the separation efficiency of a sperm sorter using a microfluidic system. First, by using 31 sperms, the sperm motion was modeled as a sinusoidal wave. The modeled sperm were supposed to move while vibrating in the fluid in the microchannel. In this analysis, the number of sperm extracted at an outlet channel and the rate of the rapid motile sperm were obtained for a wide range of flow velocities in the microchannel. By varying the channel height, sperm inlet channel width, and position, it was clarified that the separation efficiency is highly dependent on the fluid velocity in the channel. These results may be very valuable for improving the device configuration and aiming for further improvements in efficiency in the future.

1. Introduction

Sterility is often cited as one of the causes of a declining birthrate, which has become a serious social problem in recent years. Ten percent of couples have infertility problems, and almost half of all cases of sterility are associated with the lack of sperm or sperm abnormalities [1]. Motile sperm are required to increase the probability of fertilization. Processes by which motile sperm can be safely and easily sorted are therefore important for sterility treatment. Currently, the swim-up method and the density gradient centrifugal method [2] are employed for sperm sorting. However, since these methods sort sperm in a non-physiological environment, sperm damage such as DNA fragmentation is a major problem [3] and may result in the sorting of sperm that are unsuitable for fertilization.

Cho et al. [4] proposed a sperm sorter that uses a microfluidic system to extract motile sperms without causing physical sperm damage such as centrifugation. Figure 1 shows an outline of the sperm sorter with the microfluidic system. The microchannels in the device are fabricated using soft lithography methods [5]. Fluids flowing from two inlets, namely, a and b, form a laminar stream since their Reynolds numbers are very small. The laminar streams of the fluids flow in parallel without mixing with the turbulent flows at the interface between the streams to reach outlets c and d [6–11]. If a fluid containing sperm is made to flow from inlet a, nonmotile sperms and cells reach outlet c along the stream. On the other hand, some motile sperms pass through the interface to reach a different outlet, namely, d. Therefore, only motile sperms are extracted from outlet d. The flow is generated by a method that utilizes the head pressure difference produced by the difference between the amount of liquids in the reservoir chambers; therefore, as compared to conventional pump systems that are based on a mechanical method, this device is very simple

and convenient to handle. This is an important advantage, given that the device will be used by many users at various clinical sites in the future. Although a technique for extracting motile sperm has been established, the device shape or hydrodynamic conditions that enable the extraction of motile sperm with maximum efficiency have not yet been investigated. Consequently, inexpensive and immediately executable numerical simulations are required to estimate the separation efficiency of sperm sorters; further, optimally configured devices need to be investigated.

Various flagellar [12–14] models have been proposed as models for sperm motion. Since the progressive velocity and the amplitude of sperm motion are important from the viewpoint of investigating the separation efficiency of motile sperm, the present study models sperm motion as a simple sinusoidal wave, as shown in Fig. 2(a). In the simulation, the modeled sperm are arranged at either inlet of the sperm sorter to enable the sperm to move while vibrating in the fluid in the microchannel. The present paper describes how variations in the height of the microchannel and the width of the sperm inlet channel affect the number of motile sperm extracted at outlet d. In addition to the existing two-inlet, two-outlet microfluidic channel, a three-inlet, three-outlet microfluidic channel system was analyzed and the separation efficiency of motile sperm was compared between the two systems. It is hoped that the separation characteristics of the sperm sorters with microfluidic systems will be clarified through these analyses, and that the resulting information will enable the improvement of such device configurations in the future.

2. Methods

2.1 Modeling of Sperm Motion

In the present study, 31 sperms from an adult male are observed to construct a sperm motion model. The sperm motion is hypothesized to be a sinusoidal wave, as shown in Fig. 2(a). Therefore, in order to model the sperm motion, values such as the sperm velocity, amplitude of the sinusoidal wave, and period are necessary. First, an animation of 60 fps obtained by a microscope is analyzed using the digital image analysis software (MATLAB; The Mathworks, Ins.) to obtain the locus of sperm motion. Figure 2(b) shows an example of the results of tracking the motion of a sample sperm. By specifying an axis obtained by the least squares method as the X-axis, the difference between the maximum and minimum values of a Y-coordinate is defined as twice the amplitude A. Since sperms are strongly subjected to viscosity under a low Reynolds number environment, it is found that a driving force can be obtained by inducing high-speed vibrations using flagella.

A similar processing is performed for the 31 sperms, and the sperm motion is modeled based on these results. First, the length S of the sinusoidal wave shown in Fig. 2(a) is expressed as follows when applying a complete elliptic integral and using the amplitude A and the progressive length L_X of one period.

$$S = \sqrt{\left(\frac{L_X}{2\pi}\right)^2 + A^2} \; \frac{\pi}{2(1+\alpha)}\left(1+\frac{1}{4}\alpha^2\right), \qquad \alpha = \frac{\sqrt{1+k^2}-1}{\sqrt{1+k^2}+1} \tag{1}$$

Here, $k = 2\pi A/L_X$ and higher-order terms are omitted. When representing S and L_X in terms of the sperm velocity V, progressive velocity V_X, and period T used in the present analysis, the following expressions are obtained.

$$S = V\,T, \qquad L_X = V_X\,T \tag{2}$$

From the results of the analysis of the sample sperms, the sperm velocity V and period T are determined as follows:

$$V = V_{\max}\mathrm{R} \tag{3}$$
$$T = T_{\mathrm{av}} \tag{4}$$

where R denotes a random number. $V_{\max}$ denotes the maximum velocity in the sample sperms and $T_{\mathrm{av}} = 0.355$ is the average of the period of 31 sperms. Accordingly, by substituting Eqs. (2)–(4) into Eq. (1), the relation between the period A and progressive velocity V_X can be obtained. A and V_X are randomly determined within the range of the sample sperm data so as to satisfy this relation. With regard to the sperm motility, sperm whose velocity is more than half of $V_{\max}$ are judged to be rapid motile sperm.

2.2 Analysis of Sperm Motion in Microchannels

Figures 3(a) and (b) are schematic diagrams of the sperm sorters that are the subjects of the present study ((a) two-inlet, two-outlet microfluidic channel and (b) three-inlet, three-outlet microfluidic channel). In this paper, the channel branches of the inlet and outlet are not involved in the calculation region; only the portion where the flow runs in parallel was considered. This area is assumed to be a rectangular channel flow. When assuming that the x-axis is the flow direction and the yz-plane is a rectangular cross section (see Fig. 3(c)), the velocity distribution in the cross section can be theoretically obtained as follows [15]:

$$u(y,z) = \frac{16a^3}{\pi^3 \mu}\frac{\partial p}{\partial x}\sum_{n=1,3,5,\cdots}^{\infty}\frac{1}{n^3}(-1)^{\frac{n-1}{2}}\left(1 - \frac{\cosh\dfrac{n\pi y}{2a}}{\cosh\dfrac{n\pi b}{2a}}\right)\cos\frac{n\pi z}{2a}$$

$$= \frac{\pi b u_m}{2}\frac{\displaystyle\sum_{n=1,3,5,\cdots}^{\infty}\frac{1}{n^3}(-1)^{\frac{n-1}{2}}\left(1 - \frac{\cosh\dfrac{n\pi y}{2a}}{\cosh\dfrac{n\pi b}{2a}}\right)\cos\dfrac{n\pi z}{2a}}{\displaystyle\sum_{n=1,3,5,\cdots}^{\infty}\frac{1}{n^4}\left(b - \frac{a}{n\pi}\tanh\frac{n\pi b}{2a}\right)} \tag{5}$$

where u_m denotes the average flow velocity in the rectangular channel. From Eq. (5), when the shape of

the channel cross section and u_m are known, the flow velocity distribution in the channel can be obtained. Figure 3(c) shows an example of the flow velocity distribution in the cross section of the rectangular channel. The flow velocity is highest near the center and decreases as the liquid approaches the wall surface due to viscosity. Since the flow is sufficiently laminar in the actual microchannel, it is considered that the flow velocity distribution in the actual microchannel is similar to that given by Eq. (5), except in portions where the flow branches. The sperms modeled in the previous section are arranged at the upstream side of the sperm inlet channel and the sperm motion is considered as follows:

$$
\begin{aligned}
x^{t+\Delta t} &= x^t + \Delta x_s + u(y^t, z^t)\Delta t \\
y^{t+\Delta t} &= y^t + \Delta y_s \\
z^{t+\Delta t} &= z^t + \Delta z_s
\end{aligned}
\tag{6}
$$

where Δx_s, Δy_s, and Δz_s are the distances by which the modeled motile sperm moves as a sinusoidal wave along the x, y, and z directions, respectively, in Δt when there is no flow. The initial direction of the progressive velocity of the sperm is randomly specified in all directions. In the present analysis, the influence of sperm motion on the fluid and mutual interference between sperms are neglected. It is assumed that when colliding against a wall, the sperm reflect diffusely.

The microchannel length and width are fixed as $L = 5000$ μm and $W = 500$ μm, respectively. The channel height H is varied. The number of all modeled sperms that are made to flow is $N_0 = 1 \times 10^4$ and the volume of the inflow liquid is $C_f = 5$ cm^3, this number being constant. As shown in Figs. 3(a) and 3(b), the A-channel connects the sperm inlet and nonmotile sperm outlet, and the B-channel connects the sperm-free media inlet and motile sperm outlet. In the case of three-inlet, three-outlet channels, there exist two types of B-channels at the top and bottom. The width of the A-channel is W_A and that of the B-channel is W_B. The number of sperm arriving at the A-channel outlet, nonmotile sperm outlet, is N_A and the number arriving at the B-channel outlet, motile sperm outlet, is N_B. Out of N_B, the number of sperms judged to be rapid motile ($V > 0.5V_{max}$) is $N_B{}^G$. The time t necessary to make an amount of liquid (C_f) flow completely varies according to the difference in the water head pressure of the microchannel, and difference in the wettability of the channel surface. In other words, the average flow velocity in the channel varies extensively according to the device setup. Accordingly, in the present calculation, the influence of the change of H and W_A/W on N_B and $N_B{}^G$ was investigated for a wide range of flow velocities in the channel. Moreover, the difference between the two-inlet, two-outlet microfluidic channel and the three-inlet, three-outlet microfluidic channel was also examined.

3. Results and Discussion

3.1 Effect of Channel Height

First, the sperm sorting characteristics of the two-inlet, two-outlet microfluidic channel are investigated. In this section, the separation efficiency is shown when W_A/W is set to 0.25 and the height of the microchannel is varied. Figure 4(a) shows the change in the number N_B of sperms arriving at the B-channel versus the average flow velocity u_m in the microchannel. For example, when $H = 1000$ μm and

$u_\mathrm{m} = 1.0 \times 10^3$ µm/s, the Reynolds number in the channel is Re $= u_\mathrm{m}W/\nu = 0.5$, where ν denotes the kinematic viscosity ($\nu = 1.0$ mm^2/s) and the time required for 5 cm^3 of liquid to flow completely is $t = C_f/(W{\cdot}H{\cdot}u_\mathrm{m}) = 10000$ s. From the figure, it is evident that as u_m becomes slow, the number of sperms sorted into the B-channel increases. This is due to the fact that the lower u_m is, the longer the sperm will remain in the channel, and thus the probability that the motile sperm will pass through the interface between the channels increases. However, when u_m becomes lower than a certain velocity, the number of sperms arriving at the B-channel reaches a constant value since the sperms become almost uniformly distributed in the channel.

A large H causes an increase in the interface area between the two channels. However, there is almost no change in N_B between different H. That is, it is found that the probability that the motile sperms pass through the interface between channels is dependent largely on u_m rather than H. Accordingly, regardless of the channel depth, if the average flow velocity in the channel is known, the number of sperms that can be extracted into the B-channel can be estimated. In the present analysis, the amount of inflow liquid is assumed to be constant; therefore, if the volume of inflow liquid along with the channel depth is increased, N_B inevitably increases in proportion to the volume of inflow liquid and the channel depth.

The variation of $N_\mathrm{B}{}^\mathrm{G}/N_\mathrm{B}$ for wide ranges of u_m is shown in Fig. 4(b). When u_m is large, the probability that the sperm will cross the interface between channels decreases; as a result, there is a large variation in the data. Since only sperms with rapid motility can cross the interface at high u_m, the value of $N_\mathrm{B}{}^\mathrm{G}/N_\mathrm{B}$ tends to increase. On the other hand, almost no influence of differences in the channel height H on $N_\mathrm{B}{}^\mathrm{G}/N_\mathrm{B}$ is observed. Therefore, it is considered that $N_\mathrm{B}{}^\mathrm{G}/N_\mathrm{B}$ also largely depends on u_m, as well as the results of the number N_B of sperms arriving at the B-channel.

3.2 Effect of A-channel Width

The result of changing the ratio W_A/W of the width of the A-channel is shown as follows. Figure 5(a) shows the change of N_B against the average flow velocity u_m in the channel. Since the channel cross section does not change, u_m and t correspond to the scales at the top and bottom of the graph, respectively. When W_A/W is small, the average flow velocity in the A-channel is slow in comparison to the average flow velocity u_m of the entire channel. Therefore, a small W_A/W value increases the probability that the motile sperm will pass through the interface between the A-channel and B-channel, and N_B increases accordingly. On the other hand, when W_A/W is kept small, a processing limit is reached, and the sorting operation becomes difficult. Therefore, in reality, it will be necessary to maintain the channel width to some extent.

Figure 5(b) shows the ratio $N_\mathrm{B}{}^\mathrm{G}/N_\mathrm{B}$ of the number of sperms that are judged to be rapidly motile among the sperms arriving at the B-channel. Similar to Fig. 4(b), a tendency is observed wherein $N_\mathrm{B}{}^\mathrm{G}/N_\mathrm{B}$ increases with u_m. On the other hand, the average flow velocity in the A-channel decreases with W_A/W, and thus the probability that low motility sperm cross the interface increases and consequently, the rate $N_\mathrm{B}{}^\mathrm{G}/N_\mathrm{B}$ decreases with W_A/W. In summary, if a large number of sperm are required, the sperm inlet channel width should be narrowed. In contrast, the opposite treatment, namely, widening the channel width,

is effective for increasing the ratio of sperms with rapid motility among the sperms that are extracted.

3.3 Effect of the Position of the A-channel

Finally, we present the sorting characteristics of the three-inlet, three-outlet microfluidic channel, in which the A-channel is located at the center of the channel. The configuration of the three-inlet, three-outlet microfluidic channel, as shown in Fig. 3(b), is as follows. The B_1-channel and B_2-channel are fixed at the top and bottom, with the A-channel in the center. Therefore, the interface area that the A-channel contacts with the other channels is substantially larger, namely, twice that of the two-inlet, two-outlet microfluidic channel. The number of sperms to be extracted is $N_B = N_{B1} + N_{B2}$. Figure 6(a) shows the changes in the number of sperms N_B arriving at the B_1- and B_2-channels against the flow time (or average flow velocity in the channel). Upon comparing the results of the two-inlet, two-outlet microfluidic channel and those for the three-inlet, three-outlet microfluidic channel, it is obvious that N_B decreases for the same average flow velocity u_m, although the interface area is doubled in the three-inlet, three-outlet channel. These results appear contradictory; however, they are easy to understand if one considers the flow velocity distribution in the cross section of the rectangular channel shown in Fig. 3(c). Even if the average flow velocity u_m in a given channel remains the same, by arranging the A-channel at the center, the flow velocity in the A-channel becomes considerably larger than that in the two-inlet, two-outlet microfluidic channel. Consequently, the probability that motile sperms will pass through the interface is greatly reduced. Therefore, even if the interface area is doubled, N_B decreases.

Figure 6(b) illustrates a comparison of the two-inlet, two-outlet channel and the three-inlet, three-outlet channel with regard to the ratio N_B^G/N_B of sperms with rapid motility. In particular, when W_A/W is small, since the flow velocity in the A-channel is faster in the three-inlet, three-outlet channel than that in the two-inlet, two-outlet one, only rapid motile sperms can cross the interface. As a result, N_B^G/N_B increases. Therefore, it is concluded that, in the same manner as that in the two-inlet, two-outlet microfluidic channel, the most important factor with regard to the number of motile sperm is the flow velocity in the A-channel. When the flow velocity increases, the number of extracted sperm decreases; however, the ratio of the sperm with rapid motility increases. The highest priority in making the sperm sorter is to remove nonmotile sperms that are assumed to hinder fertilization and extract many motile sperms. Accordingly, based on the result of the analysis, a channel configuration that makes the flow velocity in the A-channel as slow as possible within the processing limits will be effective for increasing the number of extracted motile sperms.

4. Conclusions

In the present study, sperm modeling was conducted for the purpose of predicting the separation efficiency of a sperm sorter. Using this model, the motion of sperm in a microchannel was analyzed and the separation efficiency was investigated for various channel configurations. In conclusion, the following points were clarified.

The separation efficiency of rapid motile sperms remains almost unchanged if the average flow velocity in the microchannel remains the same. It is therefore possible to roughly predict the separation efficiency of the device by measuring the average flow velocity in the channel. As the width of the channel in which sperms flow becomes narrow, the number of extracted motile sperm increases, while the ratio of rapid motile sperms decreases. In the case of the three-inlet, three-outlet microfluidic channel, in which the A-channel is in the center, the A-channel is located at the fastest part of the rectangular channel flow velocity distribution; therefore, although the interface doubles, the number of extracted motile sperms decreases. On the other hand, the ratio of rapid motile sperms increases.

These results may serve as a very valuable prediction for improving the device configuration and developing more effective sperm sorters in the future. Since the present device requires neither electrical force nor other external forces, and handles sperms under a mechano-physiological environment, it is possible to apply it safely to cells and organisms other than sperms, such as microorganisms. It is therefore considered that the present numerical simulation can predict microorganism separation efficiency based on corresponding microorganism motion models, and it is expected to find applications in other wide-ranging applications including biomedicine.

Reference

[1] Mosher, W. D. and Pratt, W. F., "Fecundity and infertility in the United States: incidence and trends", Feritl. Steril. Vol. 56, pp. 192-193, 1991.

[2] Smith, S., Hosid, S. and Scott, L., "Use of postseparation sperm parameters to determine the method of choice for sperm preparation for assisted reproductive technology", Fertil. Steril. Vol. 63, pp. 591-597, 1995.

[3] Younglai, E. V., Holt, D., Brown, P., Jurisicova, A. and Casper, R. F., "Sperm swim-up techniques and DNA fragmentation", Hum. Reprod. Vol. 16, 9, pp. 1950-1953, 2001.

[4] Cho, B. S., Schuster, T. G., Zhu, X., Chang, D., Smith, G. D. and Takayama, S., "Passively driven integrated microfluidic system for separation of motile sperm", Anal. Chem., Vol. 75, pp. 1671-1675, 2003.

[5] Duffy, D. C., McDonald, J. C., Schueller, O. J. and Whitesides, G. M., "Rapid prototyping of microfluidic systems in poly(dimethylsiloxane)", Anal. Chem., Vol. 70, 23, pp.4974-4984, 1998.

[6] Brody, J. P. and Yager, P., "Diffusion based extraction in a microfabricated device", Sens. Actuators, A, Vol. 58, pp. 13-18, 1997.

[7] Weigl, B. H. and Yager, P., "Microfluidic diffusion-based separation and detection", Science, Vol. 283, pp. 346-347, 1999.

[8] Kenis, P. J. A., Ismagilov, R. F. and Whitesides, G. M., "Microfabrication inside capillaries using multiphase laminar flow pattering", Science, Vol. 285, pp. 83-85, 1999.

[9] Takayama, S., Ostuni, E., LeDuc, P., Naruse, K., Ingber, D. E. and Whitesides, G. M., "Subcellular positioning of small molecules", Nature, Vol. 411, pp. 1016, 2001.

[10] Tokeshi, M, Minagawa, T., Uchiyama, K., Hibara, A., Sato, K., Hisamoto, H. and Kitamori, T., "Continuous-flow chemical processing on a microchip by combining microunit operations and a

multiphase flow network", Anal. Chem., Vol. 74, pp. 1565-1571, 2002.

[11] Takayama, S., Ostuni, E, LeDuc, P, Naruse, K., Ingber, D. E. and Whitesides, G. M., "Selective chemical treatment of cellular microdomains using multiple laminar streams", Chem. Biol., Vol. 10, pp. 123-130, 2003.

[12] Higdon, J. J. L., "The hydrodynamics of flagellar propulsion: helical waves", J. Fluid Mech. Vol. 94, 2, pp. 331-351, 1979.

[13] Rikmenspoel, R., "Movement of sea urchin sperm flagella", J. Cell Biol., Vol. 76, pp. 310-322, 1978.

[14] Rikmenspoel, R., "The equation of motion for sperm flagella", Biophys. J., Vol. 23, pp. 177-206, 1978.

[15] White, F. M., Viscous Fluid Flow, 2nd ed, McGraw-Hill: New York, 1991.
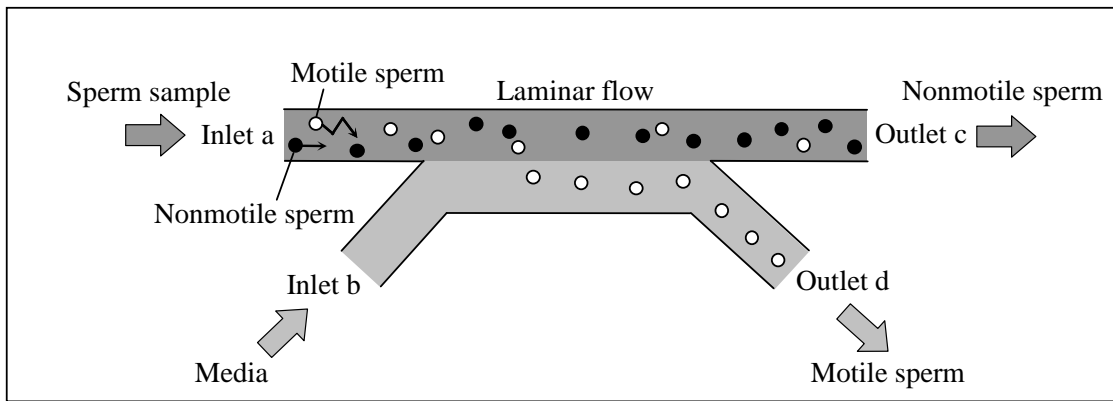
Fig. 1 Schematic diagram of a sperm sorter [5]. When a fluid containing sperms is made to flow from inlet a, nonmotile sperms and cells reach outlet c along the stream. On the other hand, some motile sperms pass through the interface to reach a different outlet, d. Therefore, only motile sperms will exit from outlet d.
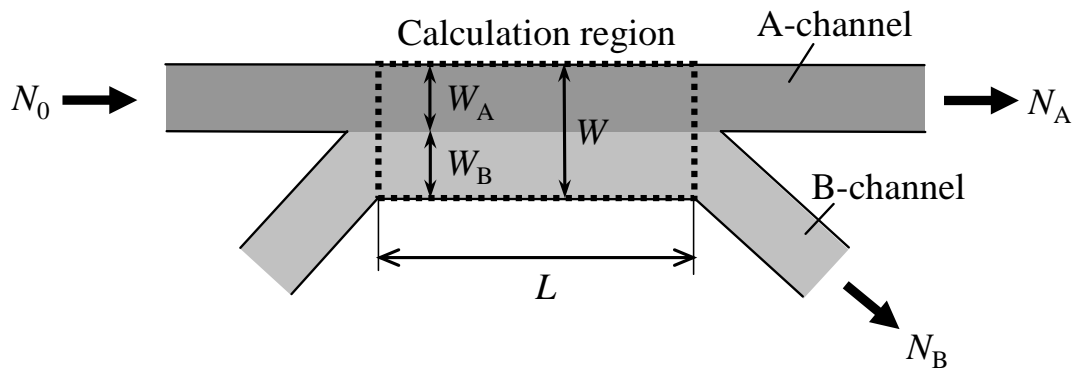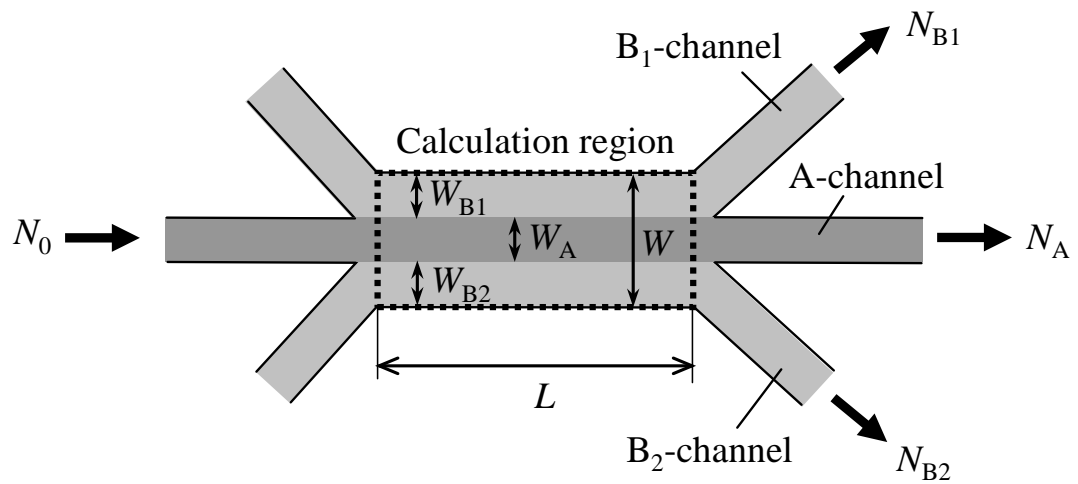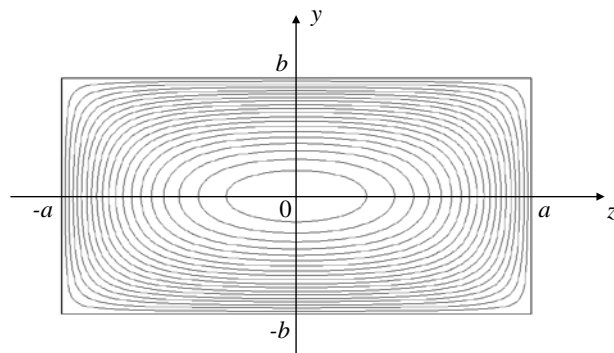
(a)   (b)
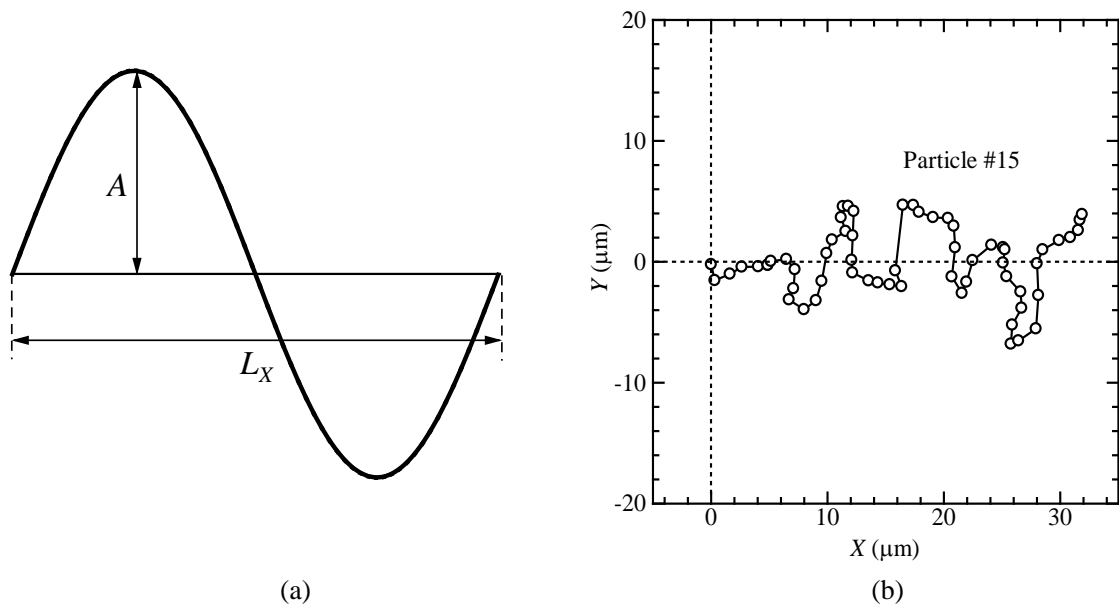
Fig. 2(a) Sperm motion is modeled as a sinusoidal wave. The amplitude is denoted by A and the progressive length is denoted by L_X. (b) The tracking of a sample sperm motion is plotted on the graph. When an axis obtained by the least squares method is specified as the X-axis, the difference between the maximum and minimum values of the Y-coordinate is defined as twice the amplitude A.

Calculation region

A-channel

N_0

W_A

W

W_B

B-channel

L

N_A

N_B

(a)

B_1-channel

N_{B1}

Calculation region

A-channel

N_0

W_{B1}

W_A

W

W_{B2}

N_A

L

B_2-channel

N_{B2}

(b)

y

b

$-a$

0

a

z

$-b$

(c)

Fig. 3(a) Two-inlet, two-outlet microfluidic channel. (b) Three-inlet, three-outlet microfluidic channel. The channel branches are not involved in the calculation region and only the portion where the flow runs in parallel is considered. The authors assume that this area is a rectangular channel flow. (c) The flow velocity distribution in a cross section of the rectangular channel is shown as an example.
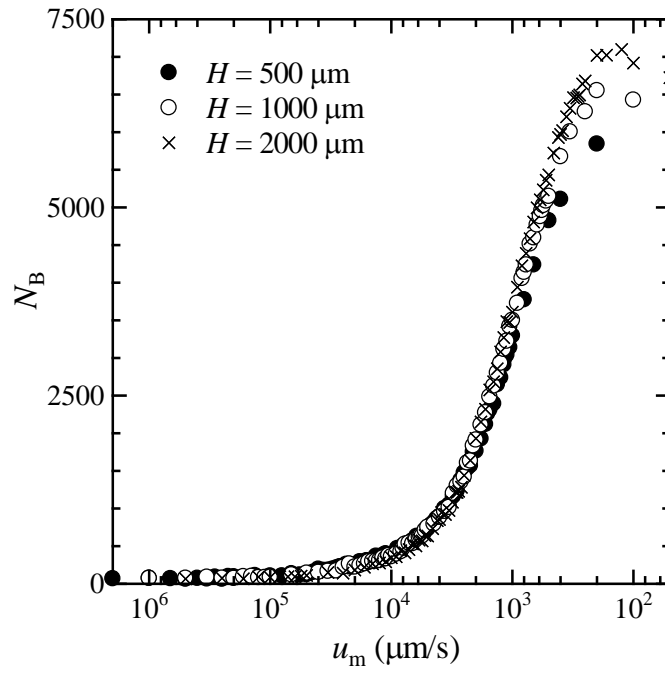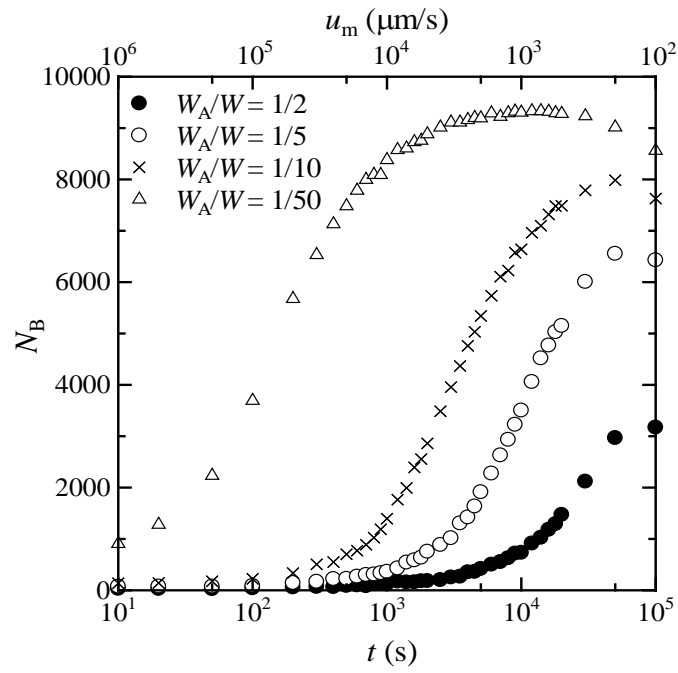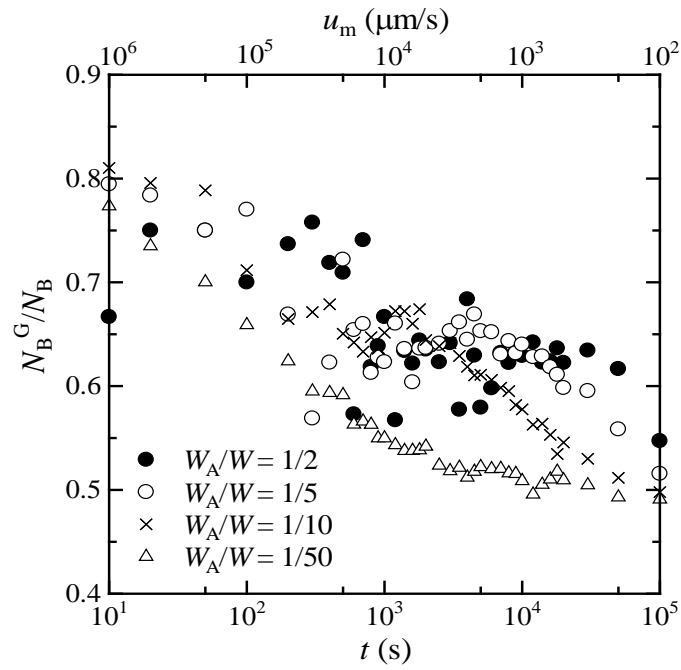
(a)
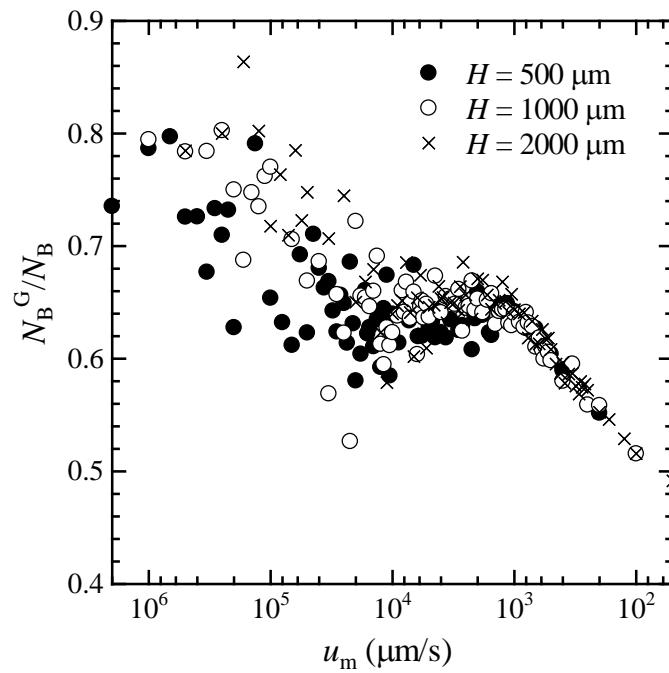
(b)

Fig. 4 The separation efficiency is shown when W_A/W is set to 0.25 and the microchannel height H is changed. (H = 500, 1000, and 2000 μm). (a) Number N_B of sperms arriving at the B-channel versus average flow velocity u_m in the channel. (b) Ratio N_B^G/N_B of the number of rapid motile sperms.
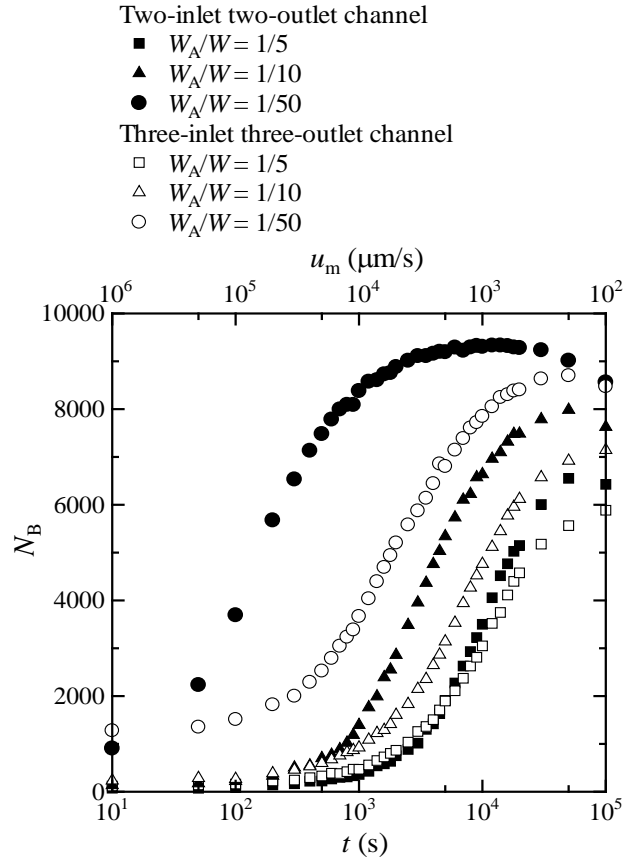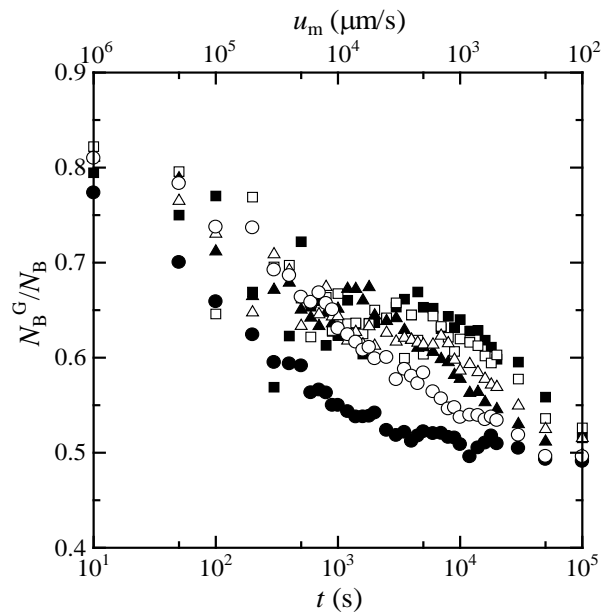
(a)

(b)

Fig. 5   The separation efficiency is shown when W_A/W (width of A-channel against channel width) is changed. ($W_A/W = 1/2$, 1/5, 1/10, and 1/50). (a) Average flow velocity u_m in the channel (or time t required for complete flow) versus number N_B of sperms arriving at B-channel. (b) Ratio N_B^G/N_B of number of rapid motile sperms.

Two-inlet two-outlet channel
- ■ $W_A/W = 1/5$
- ▲ $W_A/W = 1/10$
- ● $W_A/W = 1/50$

Three-inlet three-outlet channel
- □ $W_A/W = 1/5$
- △ $W_A/W = 1/10$
- ○ $W_A/W = 1/50$

(a)

(b)

Fig. 6   Comparison of a conventional two-inlet, two-outlet microfluidic channel and a three-inlet, three-outlet microfluidic channel, in which the A-channel is in the center. (a) Average flow velocity u_m in the channel (or time t required for complete flow) versus number N_B of sperms arriving at the B-channel. (b) Ratio N_B^{G}/N_B of number of rapid motile sperms.